A First Look at the Structure of the Wave Pouch during the 2009 PREDICT–GRIP Dry Runs over the Atlantic

ZHUO WANG

University of Illinois at Urbana–Champaign, Urbana, Illinois

MICHAEL T. MONTGOMERY

Naval Postgraduate School, Monterey, California, and NOAA/Hurricane Research Division, Miami, Florida

CODY FRITZ

University of Illinois at Urbana–Champaign, Urbana, Illinois

(Manuscript received 6 December 2010, in final form 16 August 2011)

ABSTRACT

In support of the National Science Foundation Pre-Depression Investigation of Cloud-systems in the tropics (NSF PREDICT) and National Aeronautics and Space Administration Genesis and Rapid Intensification Processes (NASA GRIP) dry run exercises and National Oceanic and Atmospheric Administration Hurricane Intensity Forecast Experiment (NOAA IFEX) during the 2009 hurricane season, a real-time wave-tracking algorithm and corresponding diagnostic analyses based on a recently proposed tropical cyclogenesis model were applied to tropical easterly waves over the Atlantic. The model emphasizes the importance of a Lagrangian recirculation region within a tropical-wave critical layer (the so-called pouch), where persistent deep convection and vorticity aggregation as well as column moistening are favored for tropical cyclogenesis. Distinct scenarios of hybrid wave–vortex evolution are highlighted. It was found that easterly waves without a pouch or with a shallow pouch did not develop. Although not all waves with a deep pouch developed into a tropical storm, a deep wave pouch had formed prior to genesis for all 16 named storms originating from monochromatic easterly waves during the 2008 and 2009 seasons. On the other hand, the diagnosis of two nondeveloping waves with a deep pouch suggests that strong vertical shear or dry air intrusion at the middle–upper levels (where a wave pouch was absent) can disrupt deep convection and suppress storm development.

To sum up, this study suggests that a deep wave pouch extending from the midtroposphere (~600–700 hPa) down to the boundary layer is a necessary condition for tropical cyclone formation within an easterly wave. It is hypothesized also that a deep wave pouch together with other large-scale favorable conditions provides a sufficient condition for sustained convection and tropical cyclone formation. This hypothesized sufficient condition requires further testing and will be pursued in future work.

1. Introduction

A longstanding challenge for both hurricane forecasters and theoreticians is to distinguish tropical waves that will develop into tropical cyclones (TCs) from tropical waves that will not. While tropical easterly waves occur frequently over the Atlantic and east Pacific, only a small fraction of these waves (~20%; e.g., Frank 1970) evolve into tropical storms. The problem was insightfully summarized by Gray (1998): ''It seems unlikely that the formation of tropical cyclones will be adequately understood until we more thoroughly document the physical differences between those systems which develop into tropical cyclones from those prominent tropical disturbances which have a favorable climatological and synoptic environment, look very much like they will develop but still do not.''

The principal reason for the difficulty of the problem is believed to lie with the multiscale nature of the tropical cyclogenesis process. The fate of a tropical easterly wave depends on the large-scale environment in which it

Corresponding author address: Zhuo Wang, Department of Atmospheric Sciences, University of Illinois at Urbana–Champaign, Urbana, IL 61801.
E-mail: zhuowang@illinois.edu

DOI: 10.1175/MWR-D-10-05063.1

Report Documentation Page

Form Approved
OMB No. 0704-0188

1. REPORT DATE	2. REPORT TYPE	3. DATES COVERED
APR 2012		**00-00-2012 to 00-00-2012**

4. TITLE AND SUBTITLE	5a. CONTRACT NUMBER
A First Look at the Structure of the Wave Pouch during the 2009 PREDICT-GRIP Dry Runs over the Atlantic	5b. GRANT NUMBER
	5c. PROGRAM ELEMENT NUMBER
6. AUTHOR(S)	5d. PROJECT NUMBER
	5e. TASK NUMBER
	5f. WORK UNIT NUMBER
7. PERFORMING ORGANIZATION NAME(S) AND ADDRESS(ES) **Naval Postgraduate School,Monterey,CA,93943**	8. PERFORMING ORGANIZATION REPORT NUMBER
9. SPONSORING/MONITORING AGENCY NAME(S) AND ADDRESS(ES)	10. SPONSOR/MONITOR'S ACRONYM(S)
	11. SPONSOR/MONITOR'S REPORT NUMBER(S)

12. DISTRIBUTION/AVAILABILITY STATEMENT
Approved for public release; distribution unlimited

13. SUPPLEMENTARY NOTES

14. ABSTRACT

In support of the National Science Foundation Pre-Depression Investigation of Cloud-systems in the tropics (NSF PREDICT) and National Aeronautics and Space Administration Genesis and Rapid Intensification Processes (NASA GRIP) dry run exercises and National Oceanic and Atmospheric Administration Hurricane Intensity Forecast Experiment (NOAA IFEX) during the 2009 hurricane season a real-time wave-tracking algorithm and corresponding diagnostic analyses based on a recently proposed tropical cyclogenesis model were applied to tropical easterly waves over the Atlantic. The model emphasizes the importance of a Lagrangian recirculation region within a tropical-wave critical layer (the so-called pouch) where persistent deep convection and vorticity aggregation as well as columnmoistening are favored for tropical cyclogenesis.Distinct scenarios of hybrid wave?vortex evolution are highlighted. Itwas found that easterlywaves without a pouch or with a shallow pouch did not develop. Although not all waves with a deep pouch developed into a tropical storm, a deep wave pouch had formed prior to genesis for all 16 named storms originating from monochromatic easterly waves during the 2008 and 2009 seasons. On the other hand, the diagnosis of two nondeveloping waves with a deep pouch suggests that strong vertical shear or dry air intrusion at the middle? upper levels (where a wave pouch was absent) can disrupt deep convection and suppress storm development. To sum up, this study suggests that a deep wave pouch extending from the midtroposphere (;600?700 hPa) down to the boundary layer is a necessary condition for tropical cyclone formation within an easterly wave. It is hypothesized also that a deep wave pouch together with other large-scale favorable conditions provides a sufficient condition for sustained convection and tropical cyclone formation. This hypothesized sufficient condition requires further testing and will be pursued in future work.

15. SUBJECT TERMS

16. SECURITY CLASSIFICATION OF:			17. LIMITATION OF ABSTRACT	18. NUMBER OF PAGES	19a. NAME OF RESPONSIBLE PERSON
a. REPORT **unclassified**	b. ABSTRACT **unclassified**	c. THIS PAGE **unclassified**	**Same as Report (SAR)**	**20**	

Standard Form 298 (Rev. 8-98)
Prescribed by ANSI Std Z39-18

is embedded, the wave's synoptic structure (e.g., low-level vorticity and middle-level moisture), and the mesoscale and convective-scale processes associated with the wave's evolution. The large-scale necessary conditions for tropical cyclone formation have been known for over four decades (e.g., Gray 1968; DeMaria et al. 2001). Using rawinsonde data, McBride and Zehr (1981) examined the differences between developing and nondeveloping cloud clusters, and showed that there is positive zonal wind shear to the north and negative zonal wind shear to the south of a developing system. They suggested that the major differences between developing and nondeveloping cloud clusters can be synthesized into a genesis potential parameter, which they defined to be the difference in relative vorticity between the upper-level (200 mb) and the low-level (900 mb) tropical flow.

Several studies in recent years have examined further developing and nondeveloping synoptic-scale precursor disturbances. Kerns and Zipser (2009) examined the vertical wind shear, midlevel mixing ratio, upper-level (200 hPa) and low-level (925 hPa) vorticity, and divergence following the tracks of individual vorticity maxima. They found that the low-level relative vorticity can best discriminate between developing and nondeveloping disturbances. Peng et al. (2012) compared developing and nondeveloping disturbances over the North Atlantic and suggested that the vertically integrated moisture, rain rate, 750-hPa relative humidity, and divergence are the most important factors in determining whether or not a tropical disturbance will develop into a tropical storm. Peng et al. found also that prior to rapid development into a tropical storm, developing disturbances may not possess stronger vorticity than their nondeveloping counterparts. In other words, at the early stage of tropical cyclone formation a developing disturbance may not be apparently different from a nondeveloping disturbance in the synoptic-scale vorticity field. Using 40-yr European Centre for Medium-Range Weather Forecasts (ECMWF) Re-Analysis (ERA-40) data and the satellite brightness temperature between 1979 and 2001, Hopsch et al. (2010) showed that the nondeveloping waves have a weaker development over the west coast of Africa and possess a more prominent dry signal just ahead of the wave trough at the middle to upper levels.

The National Aeronautics and Space Administration (NASA) African Monsoon Multidisciplinary Analyses (NAMMA) field campaign has inspired more studies on the important problem of development versus nondevelopment (Zipser et al. 2009; Vizy and Cook 2009; Ross et al. 2009; Zawislak and Zipser 2010). Ross et al. (2009) examined three African easterly waves (AEWs) in 2006 using the National Centers for Environmental Prediction (NCEP) Final Analysis (FNL). They found that the three waves all had a singular burst of diabatic heating at a particular time in the wave's history. The two developing waves were characterized by positive barotropic energy conversion (energy conversion from the mean flow to the wave disturbances). They attributed the nondevelopment of the other wave to negative barotropic energy conversion. Zawislak and Zipser (2010) found that waves with large amplitude and ''well-organized low-level circulations'' may have less precipitation and may not develop. On the other hand, they suggested that waves with ''weakly organized circulation'' may have strong vorticity centers, persistent precipitation, and better chances for development. Their study supports a distinction between the large-scale easterly wave troughs and smaller-scale vorticity centers within the wave. Their terms ''well organized'' and ''weakly organized'' appear to refer to the amplitude of the wave trough, rather than a characteristic of the tropical convection within the wave. However, a physical reason was not given by Zawislak and Zipser as to why such weakly organized waves would support more persistent precipitation and may be more likely to develop.

The different findings of the above studies may be partly due to the different tracking algorithms used and different criteria for case selection. For example, McBride and Zehr (1981) tracked cloud clusters while Kerns and Zipser (2009) tracked vorticity maxima. Peng et al. (2012) excluded disturbances with maximum relative cyclonic vorticity less than 10^{-5} s^{-1}, while Kerns and Zipser (2009) screened out disturbances lacking cold cloud-top areas in the infrared (IR) satellite data. Despite all of these analyses, the essential difference between developing and nondeveloping waves still appears to remain largely unsolved.

Recent work by Dunkerton et al. (2009, hereafter DMW09) developed a new overarching theoretical and observational framework for understanding the tropical cyclone formation processes from easterly waves. Using three independent datasets—ERA-40, Tropical Rainfall Measuring Mission (TRMM) 3B42 3-hourly precipitation, and the best-track data from the National Hurricane Center (NHC)—the Kelvin cat's eye within the critical layer of a tropical easterly wave was shown to be the preferred region of storm formation. The wave critical layer is the region of finite width surrounding the critical latitude of easterly waves in latitudinal shear flow. In the enclosed Kelvin cat's eye, air parcels tend to be trapped and recirculate, rather than being swept one way or the other by the surrounding latitudinal shear flow (DMW09). The cat's eye was hypothesized to be important to TC formation in three distinct ways: 1) wave breaking or roll-up of the cyclonic vorticity and moisture

near the critical surface in the lower troposphere provides a favored environment for the aggregation of convectively amplified vorticity; 2) the cat's eye is a region of quasi-closed Lagrangian circulation, and air is repeatedly moistened by convection and protected to some degree from dry air intrusion, which favors a predominantly convective type of heating profile; and 3) the parent wave is maintained and possibly enhanced by diabatically amplified mesoscale vortices within the cat's eye. Although the Kelvin cat's eye now serves as a canonical illustration of ''antimixing'' behavior between the cat's eye and environmental flows in the two-dimensional fluid dynamics of nonlinear waves in shear flow, this concept as applied to the equivalent barotropic representation of the mid–lower-troposphere moist critical layer of a tropical easterly wave is new.

The foregoing tropical cyclogenesis sequence and related overarching framework for describing how such hybrid wave–vortex structures develop into tropical depressions were likened to the development of a marsupial infant in its mother's pouch wherein the juvenile protovortex[1] is carried along by the mother parent wave until it is strengthened into a self-sustaining entity. The framework was therefore coined the marsupial paradigm by DMW09, and the recirculating flow in the wave critical layer was dubbed the wave's pouch, or simply, pouch. This new cyclogenesis model finds strong support in the extensive observational survey by DMW09, a recent case study of tropical cyclogenesis in the western Pacific sector during the Tropical Cyclone Structure 2008 (TCS08) field experiment (Montgomery et al. 2010b; Raymond and López Carrillo 2010), and real-case and idealized high-resolution numerical model simulations (Wang et al. 2010a,b; Montgomery et al. 2010a; Fang and Zhang 2010). A Galilean invariant ''real-time'' wave-tracking algorithm has also been developed to predict the track of possible genesis locations for real-world forecasting applications (Wang et al. 2009).

At this point it is instructive to recall that linear easterly waves and their embedded (nonlinear) critical layers generally behave differently from isolated vortices. For an isolated vortex, fluid particles in the vorticity-dominant core tend to move with the vortex, and the motion of the vortex is determined by the local steering flow and the induced azimuthal wavenumber-1 asymmetry associated with the interaction of the vortex with the environmental potential vorticity gradient and horizontal shear (e.g., Smith et al. 1990; Smith and Ulrich 1993; Reznik and Dewar 1994). By contrast, a linear easterly wave is a Rossby wave–like disturbance whose propagation is determined by the mean flow and meridional potential vorticity gradient (e.g., Thorncroft and Hoskins 1994; Holton 2004). In this case, fluid particles tend to move reversibly around their initial equilibrium position as the wave propagates through the atmosphere. The foregoing picture breaks down in the vicinity of a critical surface, wherein the wave's phase speed equals the mean flow. The embedded recirculation region (or Kelvin cat's eye flow) within the critical layer represents a locally nonlinear solution to the equations of motion at the meso-α scale. It is an intrinsic kinematic structure of the wave, instead of a direct by-product of mesoscale convection (DMW09; Montgomery et al. 2010b). The propagation properties of the cat's eye flow are governed approximately by the linear dynamics of the parent wave. This property is similar in some respects to the behavior of solitary waves (Drazin and Johnson 1989).

The wave pouch arguably provides a favorable local environment for the formation and intensification of the tropical cyclone protovortex, and the pouch center has been shown to be the preferred location for tropical cyclone formation. A more complete understanding of the kinematic, dynamic, and thermodynamic aspects of the wave's pouch is thus believed to be crucial for distinguishing developing and nondeveloping waves. An improved understanding of the pouch structure has practical benefits as well. This is because the meso-α-scale wave pouch can be resolved to some extent by coarse-resolution global model analyses and operational data, and a proper diagnosis of the wave pouch can provide useful information to hurricane forecasters.

In this paper we use the analysis and satellite data collected during the 2009 Atlantic hurricane season to examine the kinematic, dynamic, and thermodynamic structure of the wave pouch in the cyclogenesis framework developed by DMW09 (tropical cyclogenesis is defined as the formation of a tropical depression in this study). New and useful insight into the differences between developing and nondeveloping waves will be shown to emerge from this perspective.

An outline of the remaining paper is as follows: an overview of the National Science Foundation Pre-Depression Investigation of Cloud-systems in the tropics (NSF PREDICT) field campaign and the 2009 dry run is presented in section 2. Section 3 presents the data and methodology. Different wave evolution scenarios are highlighted in section 4. Section 5 presents the statistics based on 2008 and 2009 Atlantic tropical cyclones, followed by a summary and discussion in section 6.

[1] A protovortex is the initial meso-β-scale vortex within a hybrid diabatic Rossby wave–vortex, which may subsequently develop into a tropical depression–strength vortex (DMW09).

2. PREDICT field campaign and the 2009 dry run

Several field experiments on tropical cyclone formation that provided valuable observations have been carried out in the past few decades. However, the lack of in situ observations over the remote ocean that comprehensively capture the genesis processes is still one of the challenges in tropical cyclogenesis research. Without continuous observations from the pretropical depression stage (e.g., tropical wave disturbances) to the tropical storm stage, it is difficult to piece together snapshots of different individual tropical disturbances at different stages, and tropical cyclone formation remains the least understood phase of the tropical cyclone life cycle. To address the limitation of previous field campaigns, PREDICT over the west Atlantic and the adjacent seas in 2010 has increased the spatial and temporal sampling of tropical disturbances prior to, and during, genesis. The PREDICT field campaign was coordinated with the NASA Genesis and Rapid Intensification Processes (GRIP) field experiment and National Oceanic and Atmospheric Administration Hurricane Intensity Forecast Experiment (NOAA IFEX). With the National Center for Atmospheric Research (NCAR) GV aircraft and NOAA WP-3D aircraft, both synoptic and mesoscale processes that promote or hinder tropical cyclone formation have been surveyed (Montgomery et al. 2012).

To prepare for the 2010 field campaigns, the PREDICT dry run was conducted from late July through the end of September 2009, and the NASA GRIP dry run was conducted between 1 and 30 September 2009. The NOAA IFEX field experiment was also carried out in the same season. NOAA IFEX is an ongoing experiment that started in 2005 and serves as an umbrella for the NOAA Hurricane Research Division (HRD) field program each year and different items of priority. The PREDICT–GRIP–IFEX dry runs in 2009 established a useful foundation for coordination among these different project teams.

To facilitate the dry run experiments, real-time wave tracking was conducted from late July to early October in 2009. The wave pouch tracks were predicted using the algorithm developed by Wang et al. (2009) based on Global Forecast System (GFS), Navy Operational Global Atmospheric Prediction System (NOGAPS), and Met Office (UKMO) 5-day forecasts (ECMWF 5-day forecasts were added during the PREDICT field experiment). Dynamical and thermodynamic fields necessary to estimate the meso-α-scale characteristics of the wave pouch [such as vorticity, Okubo–Weiss (OW) parameter, moisture, and vertical shear] were analyzed following the propagation of the parent wave. Satellite products were examined together with the model analysis data in the marsupial framework. More than 30 waves were tracked (numbered from PG01L to PG33L over the Atlantic), 8 of which developed into tropical depressions or named storms. This study is a postanalysis of the dry run. Examples of different wave evolution scenarios are highlighted and discussed to better understand the differences between developing and nondeveloping waves.

3. Data

Five-day forecasts from three operational models, the NCEP GFS model, the NOGAPS forecast model, and the UKMO forecast model, were used for real-time wave tracking. The tracking was done once a day using the 0000 UTC forecasts and was updated twice a day using 0000 and 1200 UTC forecasts if a tropical disturbance looked favorable for development in the next 48 h. For postanalysis, the NCEP Final Analysis data from the GFS were used. The data are available at multiple vertical levels on $1° \times 1°$ grids. The data assimilation system includes observations from various satellite sensors, including Special Sensor Microwave Imager (SSM/I) precipitable water, Quick Scatterometer (QuikSCAT) surface wind, IR from the Moderate Resolution Imaging Spectroradiometer (MODIS), Meteosat, Geostationary Operational Environmental Satellite (GOES), etc. With assimilation of the observational data, the FNL analysis data provide a better representation of the atmosphere compared to GFS forecast data.

During the dry run, IR from the Naval Research Laboratory (NRL) was used for real-time wave tracking. In this study, IR images with the NHC enhancement from the Cooperative Institute for Meteorological Satellite Studies (CIMSS) Tropical Cyclone Data Archive were used for better illustration. Several other products from CIMSS were also used to examine the moisture distribution and the impacts of the Saharan Air Layer (SAL). Detailed product information can be found online at the CIMSS Web site. For completeness we give a brief description of the CIMSS products used herein.

The dry air–Saharan air layer product is created by combining the split-window imagery from GOES West and *Meteosat-8* This diagnostic product is designed to be sensitive to dry and/or dusty air in the lower troposphere (~600–850 hPa). The enhanced upper-level dry air imagery and midlevel dry air imagery are derived from the 6.2- and 7.3-μm channels on *Meteosat-8*, respectively. The former is typically most sensitive to moisture at ~400 hPa, which is above the SAL, and the latter is typically most sensitive to moisture at ~600 hPa. As shown by Dunion and Velden (2004), animations of the satellite imagery prove useful to identify the source of dry air.

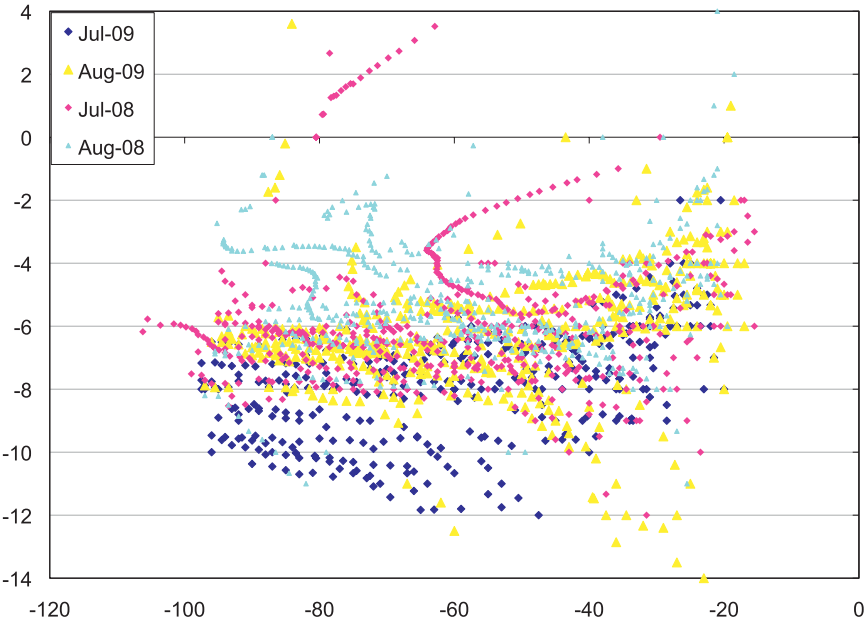

FIG. 1. Wave–storm propagation speeds (Cp) estimated from Tropical Analysis and Forecast Branch (TAFB) weather analysis. The ordinate is phase speed (° day^{-1}) and abscissa is longitude. (Courtesy of Timothy Dunkerton.)

Morphed Integrated Microwave Imagery at CIMSS–Total Precipitable Water (MIMIC–TPW; Wimmers and Velden 2007) is used to represent the total water vapor content within the air column. Disparate swaths of microwave TPW retrievals from SSM/I and the Advanced Microwave Scanning Radiometer for Earth Observing System (AMSR-E) are combined using a data-blending technique in which moisture is treated as a purely conservative tracer that is advected by a lower-tropospheric mean-layer wind derived from the GFS model. TPW measures the total water vapor in an air column and is weighted primarily to the boundary layer moisture. It therefore is unable to illustrate the vertical structure of dry air intrusion.

The enhanced IR imagery from *Meteosat-9* or GOES East and TRMM 3B42 3-hourly precipitation data are used as metrics to gauge convective activity within and outside the wave pouch. IR data have high spatial and temporal resolution but cannot easily distinguish an anvil cloud forming near the tropopause from cumulonimbus convection that spans the bulk of the troposphere.

4. Developing and nondeveloping waves in 2009

Different scenarios of hybrid wave–vortex evolution are examined based on the kinematic structure of a wave pouch: fast propagating waves without a pouch, waves with a shallow pouch confined primarily above the boundary layer or within the boundary layer, and waves with a relatively deep pouch extending from 600–700 hPa down to the boundary layer. Note that a ''deep'' pouch here is defined with respect to the lower troposphere (below 600 hPa), as a tropical easterly wave is usually confined to the lower troposphere.

a. Fast propagating waves without a pouch

Tropical cyclone activity during 2009 was below normal over the Atlantic basin. Nine tropical storms developed, three of which intensified into hurricanes. The first named storm, Ana, formed on 11 August, while on average there are two named storms formed before 6 August (see Tropical Cyclone Climatology during 1944–2005 from the NHC). Easterly waves in June–August 2009 tended to propagate faster compared to those in 2008. A large number of waves in July 2009 propagated westward 8°–12° day^{-1} (Fig. 1).[2] By contrast, the wave phase speed is typically less than 8° day^{-1} in July 2008. The typical propagation speed in August 2009 is also 1°–2° day^{-1} larger than that in August 2008. Some of the

[2] The propagation speed was estimated based on the displacement of the wave trough from its initial location when the wave was first tracked by the NHC, so large uncertainties exist in the early stage (or over the eastern part of the domain). Positive propagation speeds are associated with storms recurving eastward. Although the propagation speeds are not objectively defined, they clearly show faster propagation speeds in July 2009 (T. Dunkerton 2009, personal communication).

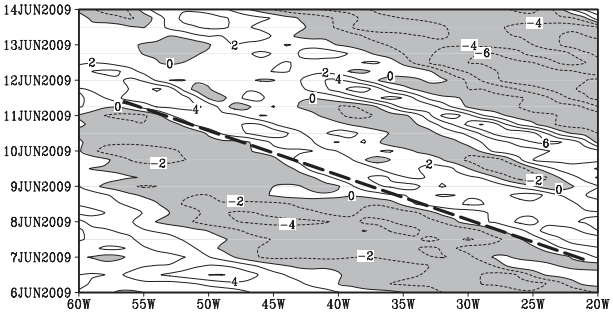

FIG. 2. Hovmöller diagram of 700-hPa meridional wind (v) along 9°N. The estimated wave propagation speed is about -10.0 m s^{-1} as indicated by the dashed sloping line.

fast propagating waves in 2009 had a large amplitude in terms of meridional extent, but they had only a small wave pouch or did not have a pouch at all. The wave propagation speeds decreased in September–October 2009 and had a similar magnitude to the phase speeds in 2008 (not shown).

An example of a fast propagating wave is shown in Figs. 2 and 3. The wave was observed over the eastern and central Atlantic in early June. The propagation speed estimated from the Hovmöller diagram of 700-hPa meridional wind is about -10 m s^{-1} (Fig. 2). In the earth-relative frame of reference, the wave had a typical inverted-V pattern in the streamline field and was embedded in the prevailing easterlies (left panels in Fig. 3). The maximum relative vorticity was approximately 3 $\times 10^{-5}$ s^{-1}. Since the wave propagation speed was higher than the total (''mean'' plus ''perturbation'') easterly flow speed, there can be no critical surface and therefore no wave pouch (or Kelvin cat's eye). In the comoving frame of reference, which moves zonally at the same speed with the wave, the zonal flow is westerly in the vicinity of the wave trough, and there is no closed circulation. Viewed within the context of the marsupial framework (DMW09), it is no surprise that this wave did not develop. Although the diagnosis of this wave is just based on model analysis data, the moral of the story is that *not every easterly wave has a critical layer or a wave pouch.*

One of the overarching tenets of the DMW09 study was that the developing waves are in fact wave–vortex hybrid systems. Our retrospective analysis suggests that some easterly waves, especially those forming early in the 2009 hurricane season, did not have a pouch. Figures 2 and 3 suggest that this was partly due to their fast propagation speeds relative to the ambient zonal flow. Another factor in the context of linear versus nonlinear waves is the wave amplitude. For these cases in which the wave's phase speed ''outruns'' the mean flow, the small but finite amplitude wind or vorticity perturbations associated with the wave usually prevent the formation of a recirculation region in the presence of sheared flow (for further discussion see DMW09).[3]

The anomalously low tropical cyclone activity of the 2009 season has been attributed largely to the developing El Niño event over the east Pacific in summer 2009, which is thought to have offset the ongoing multidecadal variations and warmer SSTs over the Atlantic (see NOAA's 2009 Atlantic Hurricane Season Outlook). The chain of events is summarized briefly as follows: the SST warming over the east Pacific affects the upper-level atmospheric circulation and leads to an enhanced vertical wind shear over the western Main Development Region (MDR; Goldenberg and Shapiro 1996). An increase in mean westerly vertical shear is thought to be one of the main agents for suppressing tropical cyclone activity over the Atlantic. It is unclear, however, how El Niño may affect tropical wave activities in the lower troposphere. Further study is necessary to understand how these types of fast propagating easterly waves may be related to the large-scale circulation and how they contribute to the variations of the tropical cyclone activity over the Atlantic.

b. *Waves with a shallow pouch*

We also observed waves with a shallow pouch in summer 2009. In these cases, a wave pouch was only present above the boundary layer (around 600–700 hPa, as usually observed over West Africa) or confined primarily within the boundary layer. The latter usually occurred for weak waves or waves in their decaying phase. The spatial size of a shallow pouch was usually small, with a radius of about 200–300 km. In some cases, they persisted for a long time and became reinvigorated in a more favorable environment (or upon interacting with other tropical disturbances). An example is Hurricane Jimena over the east Pacific (not shown), which originated from an African easterly wave (PG15L). Because of the impacts of the SAL and the associated shear deformation, the wave pouch was confined primarily around 700 hPa over the east and central Atlantic and did not extend downward below 850 hPa until the wave escaped from the impacts of the SAL to the west of 50°W (a pouch at 850 hPa was present temporarily from 1200 UTC 18 August to 0000 UTC 19 August). The wave then passed over Central America and developed into a category-4 hurricane shortly after it moved over the east Pacific.

Another example is PG07L. In this case, the pouch at 700 hPa was short-lived, lasting about 42 h, and there

[3] In principle, a sufficiently large-amplitude vorticity anomaly in the wave trough could result in a local vortex flow with recirculating air motions even if the wave propagation speed exceeds the local mean flow.

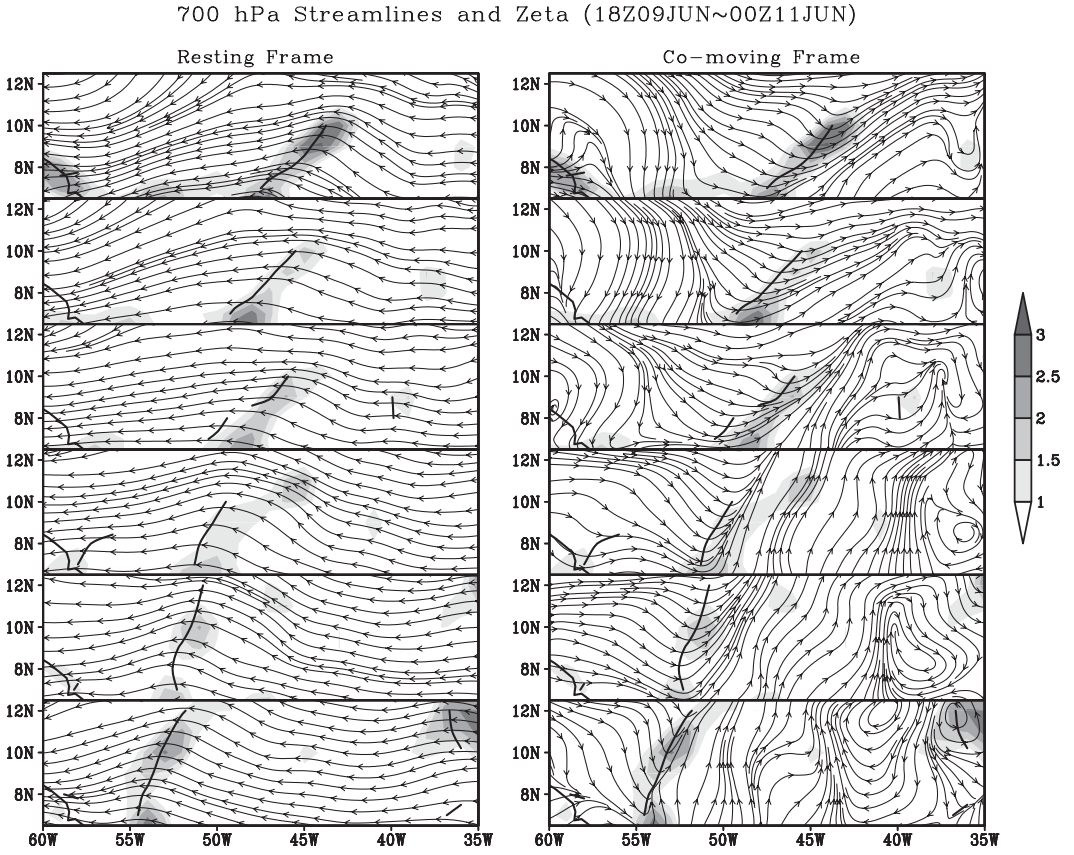

FIG. 3. Streamlines and relative vorticity (shading; 10^{-5} s^{-1}) in the (left) earth-relative and (right) wave-comoving frames of reference from 1800 UTC 9 Jun to 0000 UTC 11 Jun with the time intervals of 6 h.

was no closed circulation at 850 hPa in the wave comoving frame of reference. The maximum relative vorticity ($\sim 6 \times 10^{-5}$ s^{-1}) occurred around 700 hPa and weakened with time (Fig. 4a). Figure 4b shows the Okubo–Weiss parameter[4] [$\mathrm{OW} = \zeta^2 - S_1^2 - S_2^2 = (v_x - u_y)^2 - (u_x - v_y)^2 - (v_x + u_y)^2$]. The OW parameter is positive between 500 and 800 hPa but negative below 800 hPa. From the perspective of the meso-α-scale flow, a negative OW is consistent with the absence of a wave pouch in the lowest levels as the flow was strain rate dominant; from the perspective of the meso-β- and meso-γ-scale flow and convective organization, a negative OW region is unfavorable for sustained deep convective activity and vorticity aggregation since horizontal deformation tends to distort convective vortices irreversibly to dissipation.

c. *Developing waves with a deep pouch in the lower troposphere*

Two developing waves are discussed in this subsection: PG25L and PG20L. The former developed into Hurricane Fred close to the west coast of Africa (i.e., a Cape Verde storm), and the latter evolved into Tropical Storm Erika over the west Atlantic. Although the evolution of the two precursor disturbances is found to exhibit differences on the synoptic scale, both precursor disturbances followed the marsupial sequence, and the storms formed near the center of a wave pouch according to the GFS analysis.

1) PRE–HURRICANE FRED (PG25L)

Fred originated from an African easterly wave that moved off the west coast of Africa on 6 September. The precursor wave evolved into a tropical depression around 2100 UTC 7 September at 12.5°N, 24.5°W, about 2° south of the island of Brava in the Cape Verde Islands

[4] Assuming a scale separation between the slowly varying velocity field and the more rapidly varying field of squared vorticity (enstrophy), McWilliams (1984) and Weiss (1991) showed that positive values of OW indicate that the flow is vorticity dominant and shape preserving, whereas negative values of OW indicate a strain rate–dominated flow susceptible to rapid filamentation. A negative OW region is unfavorable for rotational organization of deep convection and aggregation of vortical remnants of prior convective activity.

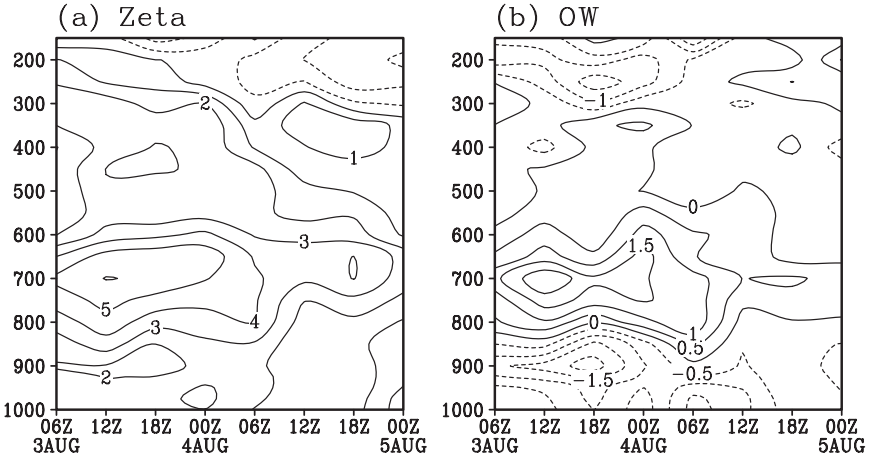

FIG. 4. Evolution of (a) relative vorticity (zeta) (10^{-5} s^{-1}) and (b) OW parameter (10^{-9} s^{-2}) averaged in a 3° × 3° box following the propagating pouch center of the PG07L disturbance at 700 hPa.

(see the corresponding 2009 NHC Tropical Cyclone Report for details). Figure 5 shows that the precursor wave propagated along the southern flank of the African easterly jet, where the background absolute vorticity is enhanced by the cyclonic shear associated with the jet. The origin of the 700-hPa wave pouch can be traced back to around 2°E, five days prior to genesis.

To understand the subsequent sequence of events in this case, it is helpful to recall that there are two wave tracks over West Africa (e.g., Carlson 1969; Reed et al. 1977), one to the north of the jet axis and the other to the south of the jet axis. The northern waves have their maximum amplitude near 850 hPa, while the southern waves have their maximum amplitude at the jet level (~600–700 hPa) (e.g., Reed et al. 1988a,b; Pytharoulis and Thorncroft 1999). The pre-Fred wave disturbance propagated along the southern wave track. Based on our experience with tracking such features, the pouch associated with a southern wave is often confined to the jet level over West Africa because of the weaker wave amplitude and the prevailing monsoonal westerly flow in the boundary layer. However, the pre-Fred wave (in the analyses) had a pouch extending downward to the 850-hPa level 2 days before the wave moved off the west coast of Africa. After the wave moved over the ocean, the wave pouch progressed downward to 950 hPa by 1800 UTC 6 September. One day later, a tropical depression formed within the cyclonic trough region of the wave disturbance.

The IR imagery superimposed on streamlines in the comoving frame of reference (Fig. 6) shows that the wave pouch was associated with active convection over

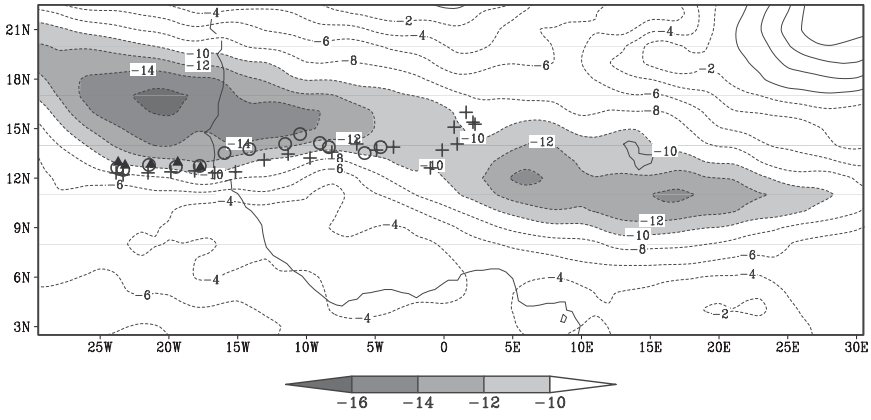

FIG. 5. The wave pouch tracks of the pre-Fred disturbance at 700 hPa (plus signs), 850 hPa (circles), and 950 hPa (triangles) from 1800 UTC 2 Sep to 1800 UTC 7 Sep with the time intervals of 6 h. Contours are 700-hPa zonal wind averaged during the same time period (easterlies stronger than 10 m s^{-1} are shaded).

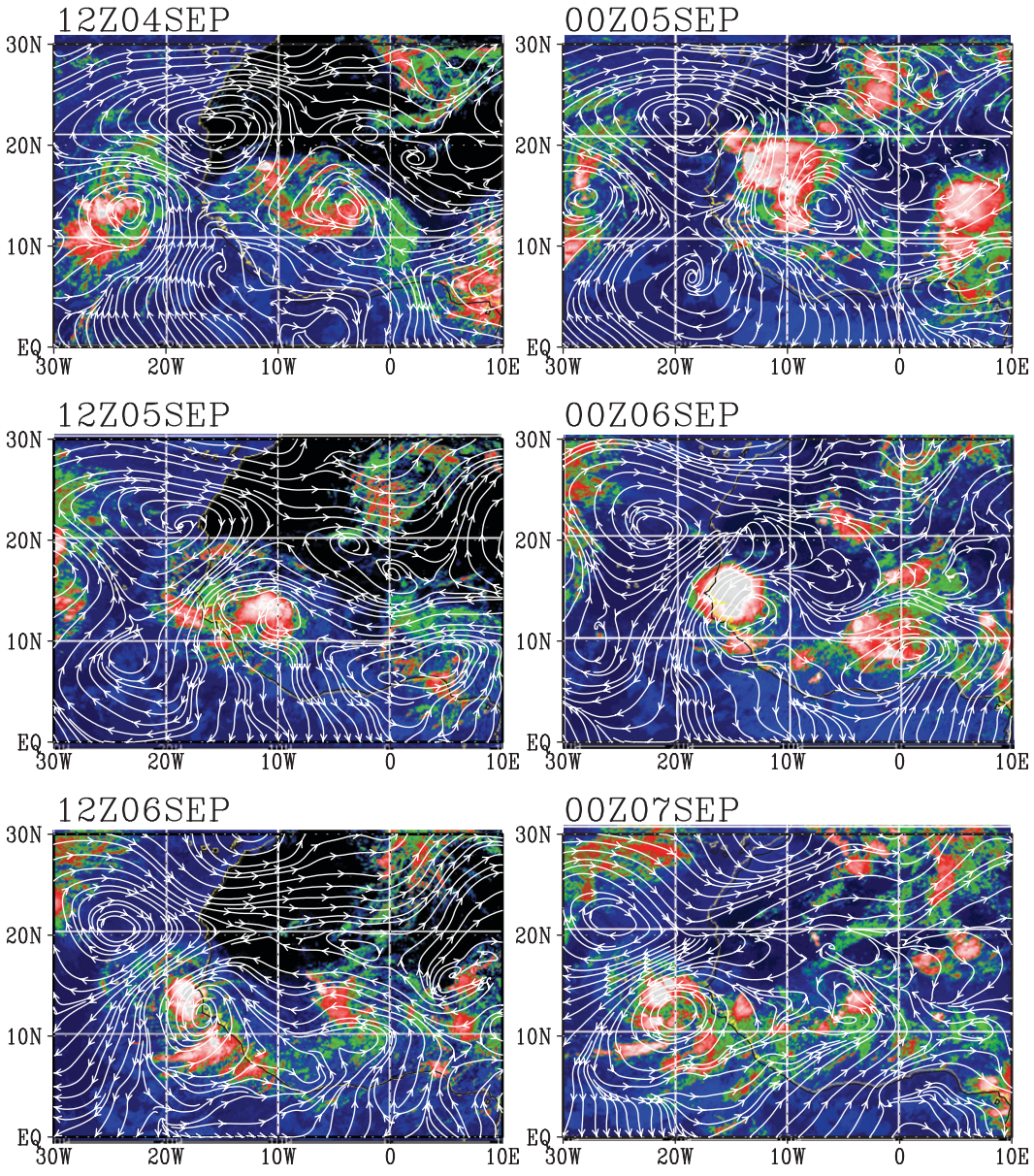

FIG. 6. Enhanced IR imagery from *Meteosat-9* superimposed on 700-hPa translated streamlines for the pre-Fred disturbance from 1200 UTC 4 Sep to 0000 UTC 7 Sep with the time intervals of 12 h. The propagation speed of the disturbance is -7.0 m s^{-1}.

West Africa. Convection was enhanced when the wave moved over the west coast (0000 UTC 6 September). After the wave moved to the ocean, the wave pouch extended down to 950 hPa (Fig. 5), and convection became organized by the cyclonic low-level circulation (last two panels in Fig. 6). The vertically coherent wave pouch and the active convection over West Africa, which moistens the wave pouch, allow for quick development of the protovortex off the coast.

An interesting question regarding the genesis of Fred is what processes contributed to the apparent downward extension of the wave pouch to the top of the boundary layer over land. Figures 7a,b show the evolution in the analyses of relative vorticity (Zeta) and divergence (Divg) averaged in a 3° × 3° box following the propagating wave pouch. The relative vorticity maximum was initially located at the jet level (~650–700 hPa), consistent with the typical vertical structure of the AEWs. There is a rapid increase of 850-hPa vorticity from 1800 UTC 4 September to 0600 UTC 5 September and a rapid increase of 950-hPa vorticity from 0600 UTC 6 September to 0000 UTC 7 September. The former is associated with the formation

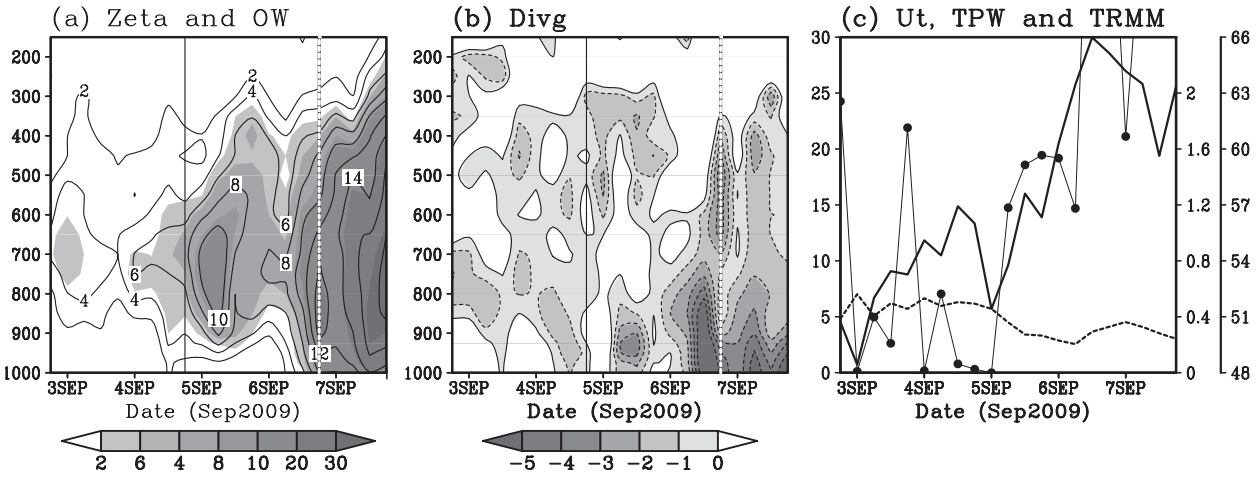

FIG. 7. Evolution of pre-Fred depicted every 6 h: (a) relative vorticity (zeta) (contours; 10^{-5} s^{-1}), OW (shading; 10^{-9} s^{-2}), (b) divergence (Divg; 10^{-5} s^{-1}), and (c) 250–850-hPa vector wind difference (Ut; dashed line with the ordinate on the left; m s^{-1}), TRMM precipitation (circles with the ordinate on the right; mm h^{-1}), and GFS TPW (solid line with the rightmost ordinate; kg m^{-2}). All variables are area averaged in a 3° × 3° box following the propagating pouch of the pre-Fred disturbance at 700 hPa. The solid (dashed) vertical line in (a) and (b) marks the time when the pouch formed at 850 (950) hPa.

of the pouch at 850 hPa, and the latter is associated with the formation of the pouch at 950 hPa. Both episodes, especially the second one, were accompanied by strong low-level convergence. As shown in Fig. 7a, the amplification and downward extension of the positive OW parameter (shading) are similar to those of the relative vorticity. We have not yet attempted to determine the minimum threshold of the OW parameter that guarantees the formation of a wave pouch. However, positive OW is clearly a necessary condition.

In the presence of sustained low-level convergence, the material form of the vorticity equation (Pedlosky 1987) implies that cyclonic vorticity tends to increase as parcels move into the region of convergence. The evolution of the pre-Fred disturbance suggests that low-level convergence enhances the low-level cyclonic vorticity and the OW parameter, an interpretation that is consistent with recent work (e.g., Wang et al. 2010a; Montgomery et al. 2010b; Raymond and López Carrillo 2010). This low-level spinup process generates a low-level pouch in the comoving frame with strong rotation and weak strain rate in the presence of westerly relative flow.

Figure 7c shows the 250–850-hPa vertical wind shear, total precipitable water, and precipitation rate from TRMM 3B42. The vertical shear in the deep troposphere was less than 7 m s^{-1} throughout the calculation time period, which should not significantly disrupt the occurrence of persistent deep convection. On the other hand, recent studies have suggested that deep convection can act to reduce the vertical wind shear across the troposphere (e.g., Davis and Bosart 2003; Hendricks and Montgomery 2006).

Figure 7c shows that TPW and TRMM precipitation increased significantly from 0000 UTC 5 September to 1200 UTC 6 September. The increase of total precipitable water in the air column can be attributed to convection, which converges moisture in the boundary layer and moistens the middle and upper troposphere. High moisture content is currently thought to provide a favorable condition for persistent convection by reducing the import of air with low equivalent potential temperature into the boundary layer.[5]

2) PRE–TROPICAL STORM ERIKA (PG20L)

The pre-Erika disturbance can be traced back to West Africa around 2°E at 0000 UTC 23 August (Fig. 8). In the analysis data, the wave pouch was confined to a relatively shallow layer between 600 and 700 hPa. After departing from land, the analyzed pouch extended down to 850 hPa (but not 950 hPa). However, the OW parameter was rather weak at 850 hPa before 0000 UTC 27 August (~1 × 10^{-9} s^{-2}; middle panels in Fig. 9). Although the pouch was centered at 15°N, the wave trough extended southward to the ITCZ. This wave trough appeared to stimulate a convective system around 10°N (indicated by TRMM precipitation in the bottom panels in Fig. 9). A new disturbance with a cyclonic gyre

[5] However, recent evidence from state-of-the-art numerical cloud models suggests that the presence of midlevel dry air is not to strengthen downdrafts, but rather to reduce the strength of updrafts by weakening both updrafts and downdrafts (James and Markowski 2010; Kilroy and Smith 2011, manuscript submitted to *Quart. J. Roy. Meteor. Soc.*).

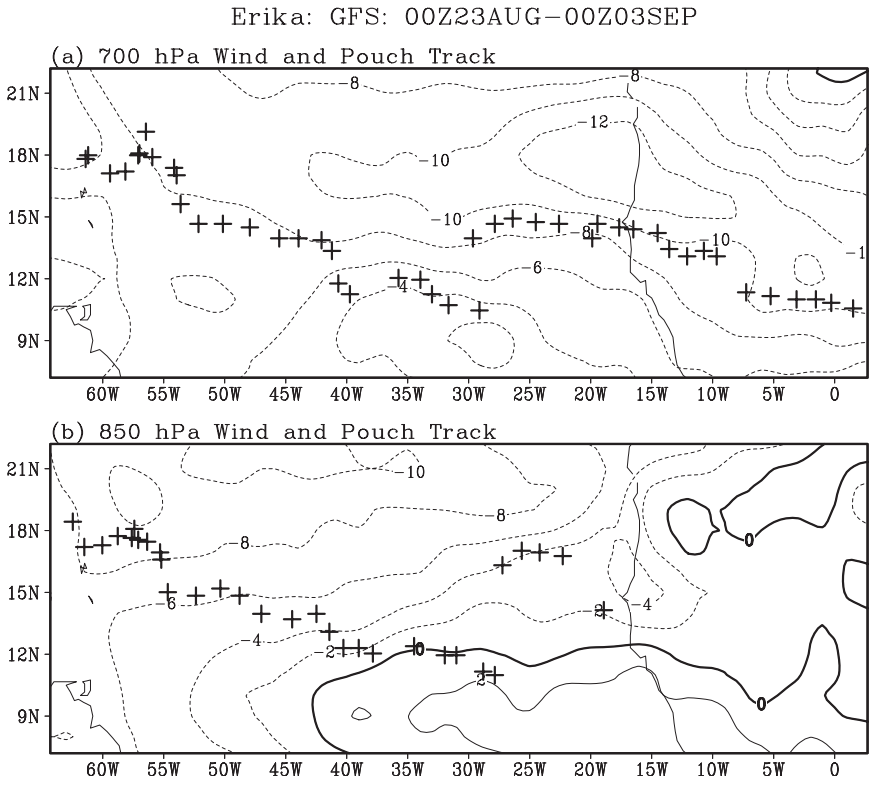

FIG. 8. The (a) 700- and (b) 850-hPa wave pouch tracks (plus signs) for the pre-Erika disturbance superimposed on the zonal flow averaged from 0000 UTC 23 Aug to 0000 UTC 3 Sep. (Note that the 850-hPa wave pouch did not exist before 1200 UTC 26 Aug.)

appeared around 10°N by 1200 UTC 27 August, and the AEW to the north of this disturbance began to weaken. It is informative to note that the AEW and the ITCZ disturbance initially have peak amplitudes at different vertical levels in the analysis data: the former has maximum OW and a well-defined pouch at 700 hPa, and the latter has stronger OW at 850 hPa and below. The two cyclonic disturbances then rotate counterclockwise around their interior vorticity centroid, much like point vortices with circulations of the same sign (Fujiwhara 1921; McWilliams 2006). Meanwhile, the initial wave pouch becomes larger at 700 hPa and progresses downward to 950 hPa (the bottom panels in Fig. 9). The pouch also shifts southward toward the ITCZ, a region of enhanced moisture. GFS analysis suggests that the AEW and the ITCZ disturbances appear to merge. The resulting composite disturbance continues to propagate westward and subsequently develops into Tropical Storm Erika after escaping from the negative impacts of strong vertical wind shear.

This wave–ITCZ interaction is evident also in the IR Hovmöller diagrams (Fig. 10). The AEW was associated with scattered convection near Dakar, Senegal, on 25 August. Convection became stronger on 26 August and extended southwestward to the ITCZ region. As its northern portion died out, the convective system developed a more circular pattern around 10°N, which continued to propagate westward in the subsequent couple of days.

An interesting feature of the wave–ITCZ interaction is that the convective burst shown in the IR Hovmöller diagram (Fig. 10) or TRMM precipitation (bottom panels in Fig. 9) occurred before the formation of the 950-hPa wave pouch. TRMM precipitation also shows that new convective cells in the ITCZ region tend to form ahead of the 700-hPa wave trough axis, where moisture convergence is enhanced by the northerly perturbations associated with the AEW. Although global model analysis data have a limited capability in resolving subsynoptic-scale processes, Figs. 9 and 10 depict a plausible sequence for the ITCZ–wave interaction: an African easterly wave a few degrees north of the ITCZ enhances moisture convergence in the ITCZ region and stimulates deep convection ahead of the wave trough; the associated lower-tropospheric convergence gradually spins up a low-level cyclonic gyre; the interaction between the low-level disturbance in the ITCZ region and the somewhat elevated easterly wave disturbance to the north results in

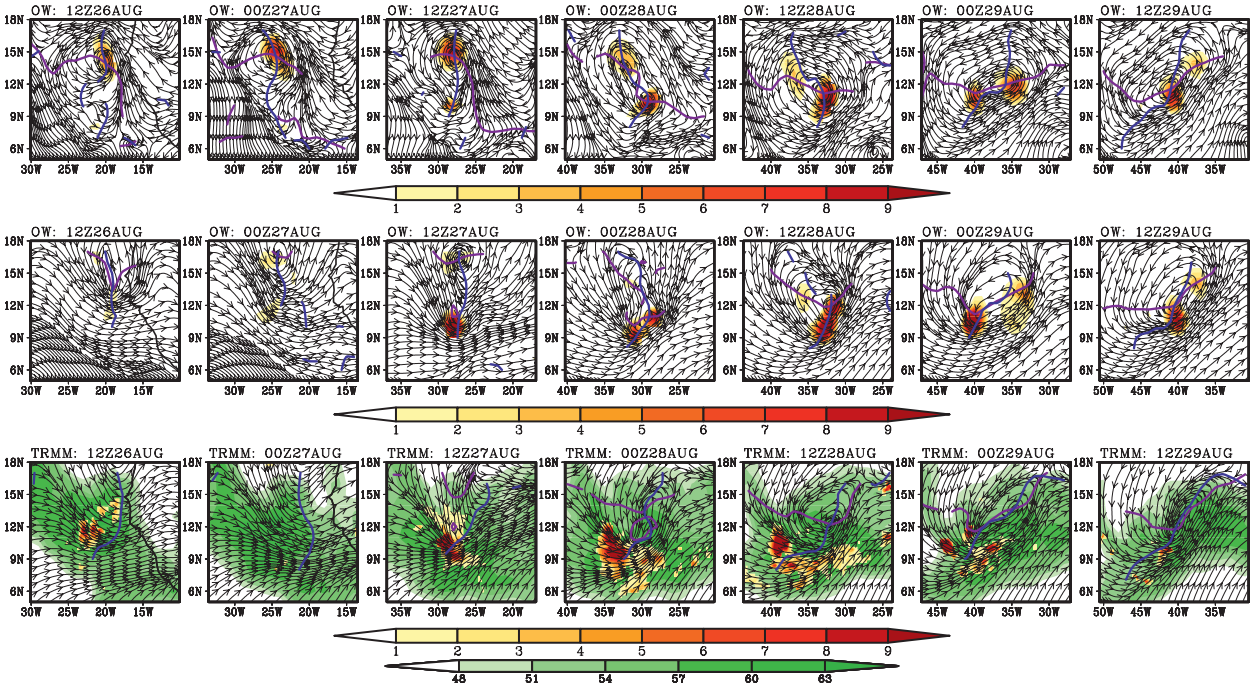

FIG. 9. Evolution of the pre-Erika disturbance. The (top) 700- and (middle) 850-hPa streamlines in the comoving frame of reference and OW parameter (10^{-9} s^{-2}); (bottom) 950-hPa streamlines in the comoving frame, TRMM precipitation (yellow shading; mm h^{-1}), and TPW (green shading; kg m^{-2}). The blue curve indicates the wave trough axis, and the purple curve represents the wave's local critical latitude. The zonal propagation speed of the parent easterly wave is −8.5 m s^{-1} (estimated from a Hovmöller diagram of the meridional wind).

a more vertically coherent (deeper) pouch structure, which is more conducive for tropical cyclone formation than from either disturbance alone. The evolution of the pre-Erika disturbance as viewed in the analyses suggests that convection can influence the wave intensity, propagation speed, and even the track. On the other hand, we would like to point out that the African easterly wave played an essential role in the evolution shown in Fig. 9: 1) the convection in the ITCZ region is likely stimulated by the wave; 2) the ITCZ disturbance developed within the pouch of the African easterly wave at 700 hPa, and this disturbance may not last long enough to spin up a tropical depression vortex without the wave pouch above the boundary layer. We note also that the horizontal tilt of the wave pouch changes with time (most pronounced at 700 hPa). When it tilts against the horizontal shear of the mean flow (from 0000 to 1200 UTC 29 September), simple dynamical arguments would suggest that the wave extracts energy from the mean flow.

It is useful to point out that the new model for tropical cyclogenesis from easterly waves (DMW09) embraces two principal pathways for tropical cyclogenesis that are relevant to understanding this wave–ITCZ interaction. In the first pathway, the isolated wavelike disturbance on the ITCZ would act to excite a quasi-neutral cat's eye circulation at the wave's critical latitude on the northern side of the ITCZ. The downstream propagation of easterly waves and the ensuing convective development within this cat's eye may provide an efficient route to tropical cyclogenesis even if the waves are stable or quasi-neutral. For an ITCZ mean flow that supports a nontrivial exponential instability, the easterly wave–like disturbance in the first pathway would amplify exponentially in the ITCZ. However, once such a disturbance attains sufficient amplitude, it is an equally good candidate to support cyclogenesis within a critical layer as a neutral wave.

d. Nondeveloping waves with a deep pouch in the lower troposphere

Tropical easterly waves usually have a maximum amplitude at the jet level (600–700 hPa over the east Atlantic and 850 hPa or lower over the west Atlantic). A deep pouch extending throughout the lower troposphere provides a connection between the free atmosphere and the boundary layer, the ultimate moisture source for the interior. Such a vertically coherent structure arguably provides a favorable local environment for tropical cyclone formation, as 1) it helps to contain moisture lofted from deep convection or laterally entrained from nearby sources (e.g., the ITCZ) within the pouch and to protect

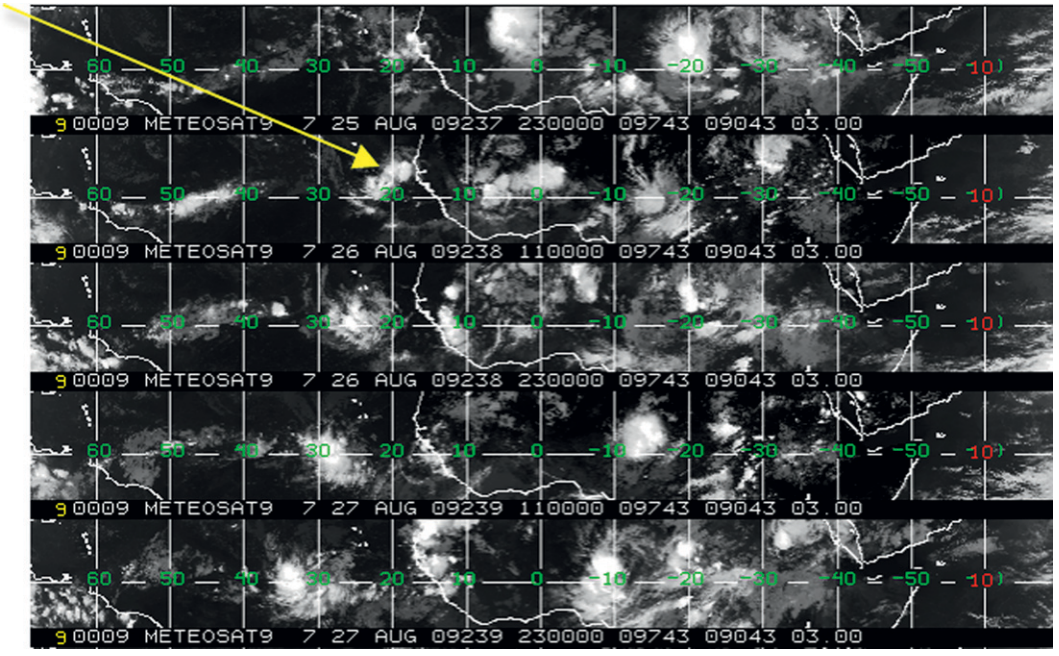

FIG. 10. Hovmöller diagram of IR. The yellow arrow highlights the convective burst in the ITCZ region catalyzed by the AEW. The arrow highlights the wave–ITCZ convection composite. (Figure adapted from the NHC.)

the moist air within from dry air intrusion; 2) the quasi-circular cat's eye circulation on the meso-α scale in the lower troposphere acts as a ''guiding hand'' for the organization of meso-γ-scale convective cells and their vortical remnants, and the associated secondary (overturning) circulation within the cat's eye accelerates the construction of the meso-β-scale protovortex at the pouch center (Wang et al. 2010 a,b; Montgomery et al. 2010a; DMW09). Our preliminary results based on real-time wave tracking in the 2008 and 2009 hurricane seasons showed that all tropical cyclones originating from monochromatic tropical easterly waves formed from a deep pouch (see more details in section 5) and suggest that a deep wave pouch may be a necessary condition for tropical cyclone formation. However, a deep wave pouch by itself does not guarantee tropical cyclone formation. Tropical waves PG24L and PG26L are two examples of nondeveloping waves with a deep pouch and are discussed in the following two subsections.

1) PG24L

Similar to the pre-Fred disturbance, the easterly wave PG24L was convectively active over West Africa, and the wave pouch extended down to 850 hPa around 5°E (Fig. 11). The wave disturbance was associated with strong positive relative vorticity in the lower and middle troposphere, with a maximum of about 1.5×10^{-4} s^{-1} at 550 hPa on 3 September (Fig. 11a). The OW maximum is about 1.8×10^{-8} s^{-2} at the same level (shading in Fig. 11a). The GFS analysis suggests that there was persistent low-level convergence, especially from 2 to 5 September (not shown). However, the wave experienced strong vertical shear after 0000 UTC 6 September (exceeding 25 m s^{-1}) (Fig. 11c). An increase in vertical wind shear was accompanied by a drop in relative humidity in the middle–upper troposphere, which first took place at 300–600 hPa and later extended below 700 hPa (Fig. 11b). TPW and TRMM precipitation decreased as well (Fig. 11c). The IR imagery (not shown) indicates that convection weakened and became disorganized after 6 September. These facts point to the intrusion of dry air into the pouch region, which would tend to frustrate convective development.

Figure 12 shows the track of the 850-hPa wave pouch from 0000 UTC 1 September to 0000 UTC 9 September. After the wave departed West Africa, it turned northwestward to a region of low TPW. Along the pouch track, the easterly flow increased at 850 hPa while the easterly flow decreased at 250 hPa, and the wave pouch eventually propagated into the region of strong upper-level westerly flow. The primary contribution to the strong vertical wind shear (Fig. 11c) comes from the zonal wind. The streamlines in the comoving frame of reference (not shown) show that the wave pouch was ripped open at 500 hPa on 5 September, leaving the low-level pouch vulnerable to midlevel dry air intrusion. The 850-hPa wave pouch, however, persisted until the wave propagated under the upper-level westerly jet.

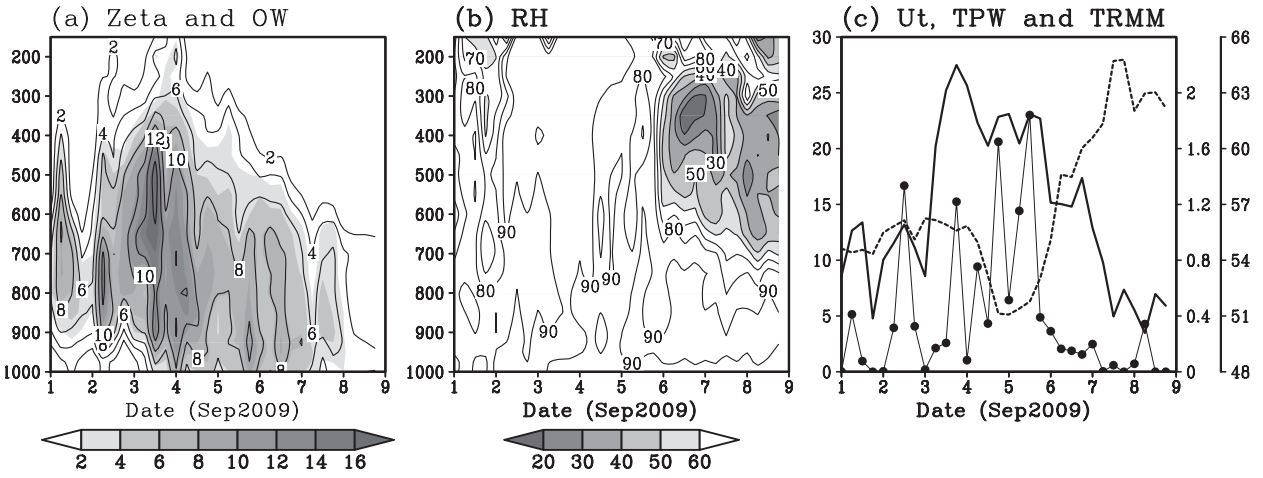

FIG. 11. (a),(c) As in Figs. 7a,c, but for PG24L. (b) Evolution of RH (%). The abscissa is dated from 0000 UTC 1 Sep to 0000 UTC 9 Sep.

It has been known for several decades that strong vertical shear is detrimental for tropical cyclone formation, but the impacts of vertical shear on a wave pouch are not well understood. For PG24L, a well-defined pouch in the lower troposphere extending from 700 to 950 hPa existed until 0000 UTC 8 September. Subsequently, the pouch was ripped open at 700 hPa at 0600 UTC 8 September and ripped open at 850 and 950 hPa at 0000 UTC 9 September. At times during the lifetime of the wave pouch, the vertical shear exceeded 20 m s^{-1}. Evidently, a wave pouch is somewhat resilient to deep vertical shear. This may be partly due to the vertical structure of the wave pouch, which tends to be confined in the mid–lower troposphere and may be less sensitive to the vertical shear over the deep troposphere than a tropical storm extending through the full troposphere (the strong vertical shear occurred between 600 and 200 hPa in this case). In addition, a wave pouch is also much different from an individual vortical convective element because it has a much larger horizontal scale and can be distorted and tilted to some extent under the impacts of vertical shear.

A vertically aligned pouch is thought to be favorable for tropical cyclogeneisis because an aligned pouch implies a strong vortex resilience (Jones 1995; Reasor et al. 2004). DMW09 showed that vertical tilted pouches tend to become more vertically aligned around the genesis time. This may, in part, result from persistent convection in a rotating background flow whose aggregate effect is to converge absolute vorticity throughout a deep layer. In some cases, the vertical shear may also help to bring a tilted pouch, which is due to slightly different propagation speeds at different vertical levels, into vertical alignment. The latter is consistent with some previous studies that suggested that weak but nonzero vertical shear may be conducive to tropical cyclone formation (e.g., Bracken and Bosart 2000). Although PG24L did not develop into a tropical storm, the western North Pacific case study by Montgomery et al. (2010a) suggested that a wave pouch survived in the presence of strong vertical shear (exceeding 21 m s^{-1}) and later developed into Typhoon Nuri (2008) as the vertical shear abated to weaker values in the vicinity of the pouch.

2) PG26L

PG26L was also an AEW. It had a deep wave pouch extending from 700 to 950 hPa that lasted about 10 days (13–24 September) (the pouch first formed at 950 hPa, instead of at 700 hPa, and there was no well-defined pouch at 500 hPa and above). The wave was designated as an invest (98L) by the NHC on 18 September, but it was dropped two days later. Figure 13 shows the evolution of vorticity, OW, relative humidity, vertical shear, TPW, and TRMM precipitation averaged in a 3° × 3° box following the propagating wave pouch. Area-averaged relative vorticity was on the order of 10^{-4} s^{-1} and confined to the lower troposphere (mainly below 700 hPa). Vertical shear between 250 and 850 hPa was less than 10 m s^{-1} before 20 September and less than 15 m s^{-1} after 20 September. What suppressed further development of the wave was likely the upper- and midlevel dry air intrusion from 17 to 24 September. GFS analysis data show that the air was very dry from 300 to 600 hPa, and relative humidity was as low as 20%. At 700 hPa, dry air was spiraled into the pouch because of the convergent flow (not shown), and TPW decreased gradually from 58 to 48 kg m^{-2} during 18–23 September. Although there was intermittent convection within the pouch at the early

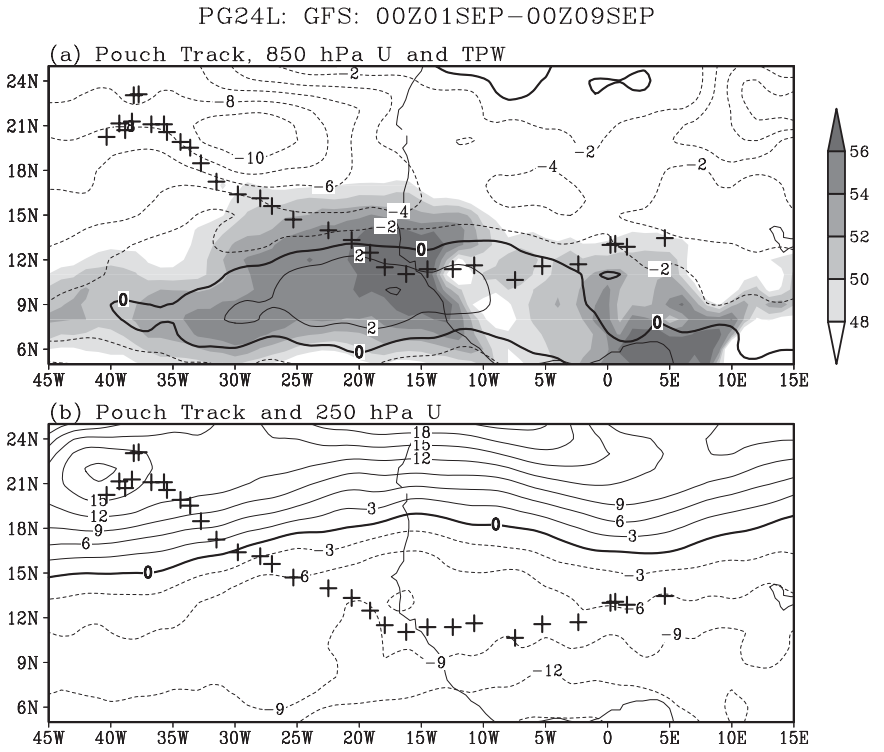

FIG. 12. The 850-hPa pouch track for PG24L superimposed on (a) 850- and (b) 250-hPa zonal wind averaged from 0000 UTC 1 Sep to 0000 UTC 9 Sep. The thick curves are the zero contours. The contour intervals are (a) 2 and (b) 3 m s^{-1}. Shading in (a) is the TPW (kg m^{-2}) in the column from the GFS analysis.

stage, convective activity diminished significantly after 19 September.

Because of the coarse resolution and the cumulus parameterization used in the atmospheric model, GFS analysis data may not adequately represent the moisture profile. Satellite observations are used here to offer a preliminary assessment. Figure 14a shows the MIMIC–TPW superimposed on 850-hPa translated streamlines at 1800 UTC 18 September. A well-defined wave pouch was present at 850 hPa. The pouch was moist except in the western and northwestern quadrants. As a vertically integrated quantity, TPW cannot distinguish midlevel dryness from low-level dryness. The enhanced midlevel water vapor imagery (Fig. 14b) and upper-level (Fig. 14c) water vapor imagery show that the midlevel and upper-level air was dry to the north and to the west of the wave pouch. The dry and dusty air associated with the SAL, however, was relatively weak at this time (Fig. 14d). Also, note that the vertical cross section in Fig. 13 suggests that strong dry air intrusion occurs between 300 and 600 hPa, which is above the SAL (e.g., Diaz et al. 1976; Karyampudi et al. 1999). An animation of the satellite imagery during 15–18 September suggests that the dusty and dry air in the lower troposphere (highlighted in Fig. 14d) originated from West Africa, while the mid- to upper-level dry air mass came from the north, associated with a midlatitude front.

Figure 15 shows the 600-hPa geopotential height (black contours), relative humidity (green contours), and vertical velocity (shading) in the isobaric coordinates averaged temporally between 0000 UTC 17 September and 0000 UTC 24 September. The dominant features in the geopotential height field are the subtropical high over the North Atlantic, the anticyclone over North Africa, and a trough in between. Strong subsidence occurred between the Atlantic subtropical high and the trough. The midlevel dry air, as highlighted by 600-hPa relative humidity less than 50%, covered a large portion of the North Atlantic and extended southward beyond 15°N and between 40° and 60°W. The dry air is mostly collocated with subsidence, and this suggests that the dry air is at least partly due to the large-scale subsidence, which is consistent with Braun (2010). To examine the source of the midlevel dry air, a 2D (horizontal) trajectory analysis was conducted at 500 hPa (Fig. 15). The trajectories show that some parcels in the western part of the wave indeed originated from the midlatitude dry air mass to the north.

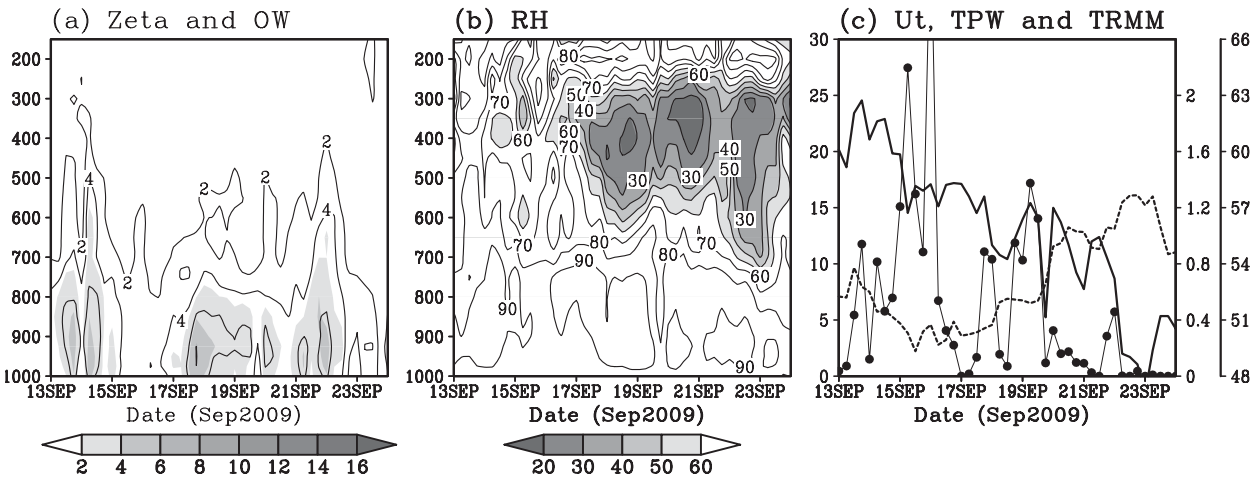

FIG. 13. Same as Fig. 11, but for PG26L. The abscissa is dated from 0000 UTC 13 Sep to 0000 UTC 24 Sep.

5. Statistics

To further test the hypothesis that a deep pouch extending throughout the lower troposphere is a necessary condition for tropical cyclone formation, we examined the tropical storms originating from quasi-monochromatic tropical easterly waves over the Atlantic from June to October 2008 and 2009. [For simplicity, we excluded the storms forming from subtropical frontal zones (Grace in 2009, and Christobal, Edouard, and Laura in 2008) and those tracking northward or northwestward (Kyle in 2008 and Claudette in 2009)]. There were 6 such storms in 2009 and 10 in 2008. Figure 16 shows the lifetime of the wave pouches at different vertical levels prior to genesis (genesis is defined as the first tropical cyclone point appearing in the NHC best-track data). In all 16 storms, a deep wave pouch extending from 700 to 950 hPa had formed at least 24 h before genesis. In 10 of these storms, a pouch formed at 700 hPa first (or concurrently with an 850-hPa pouch) and then progressed downward. This type of wave pouch development tends to occur from June to September. The second type of wave pouch development, in which a wave pouch first formed at either 850 or 950 hPa, tends to occur in the late season (i.e., October). It is interesting to note that the deep pouch lifetime prior to genesis varies from about 7 days (Fay 2008) to 24 h (e.g., Danny). The fact that it may take 6–7 days for a tropical storm to form within a deep pouch suggests that a deep pouch by itself is just a necessary condition for tropical cyclone formation and that other factors that affect the diabatic activation of the wave pouch, such as SST, vertical wind shear, and upper- to midlevel dry air, may have delayed the development of a tropical storm.

Among the 16 storms selected above, Bertha (2008), Ike (2008), Josephine (2008), Nana (2008), Ana (2009), Bill (2009), and Fred (2009) are Cape Verde storms and formed to the east of 40°W. According to the analysis, all of these storms except Nana (2008) possessed a wave pouch extending from 700 to 850 hPa before they moved off the West African coast. The closed circulation between 700 and 850 hPa allows quick development of the precursor waves after they move to the warm ocean, if other environmental conditions are favorable. The formation sequence of Fred may be typical for Cape Verde storms.

6. Summary and discussion

A real-time wave-tracking algorithm based on the marsupial paradigm was applied to tropical easterly waves in the Atlantic basin during the 2009 NSF PREDICT dry run. The dry run was carried out in collaboration with the NASA GRIP dry run and NOAA IFEX. More than 30 waves were tracked from late July to early October, and 8 of them developed into a tropical depression or a named storm. Using GFS analyses and satellite data, this study identified four different wave evolution scenarios: 1) fast propagating waves without a wave pouch, 2) waves with a shallow pouch confined primarily above the boundary layer or within the boundary layer, 3) waves with a deep pouch extending over the entire lower troposphere that developed, and 4) waves with a deep pouch that did not develop.

Easterly waves without a pouch or with a shallow pouch did not develop. Although not all waves with a deep pouch developed into a tropical storm, our diagnoses showed that a deep wave pouch had formed at least 24 h prior to genesis in all 16 named storms that originated from monochromatic tropical easterly waves over the Atlantic during June–October 2008–2009. Our

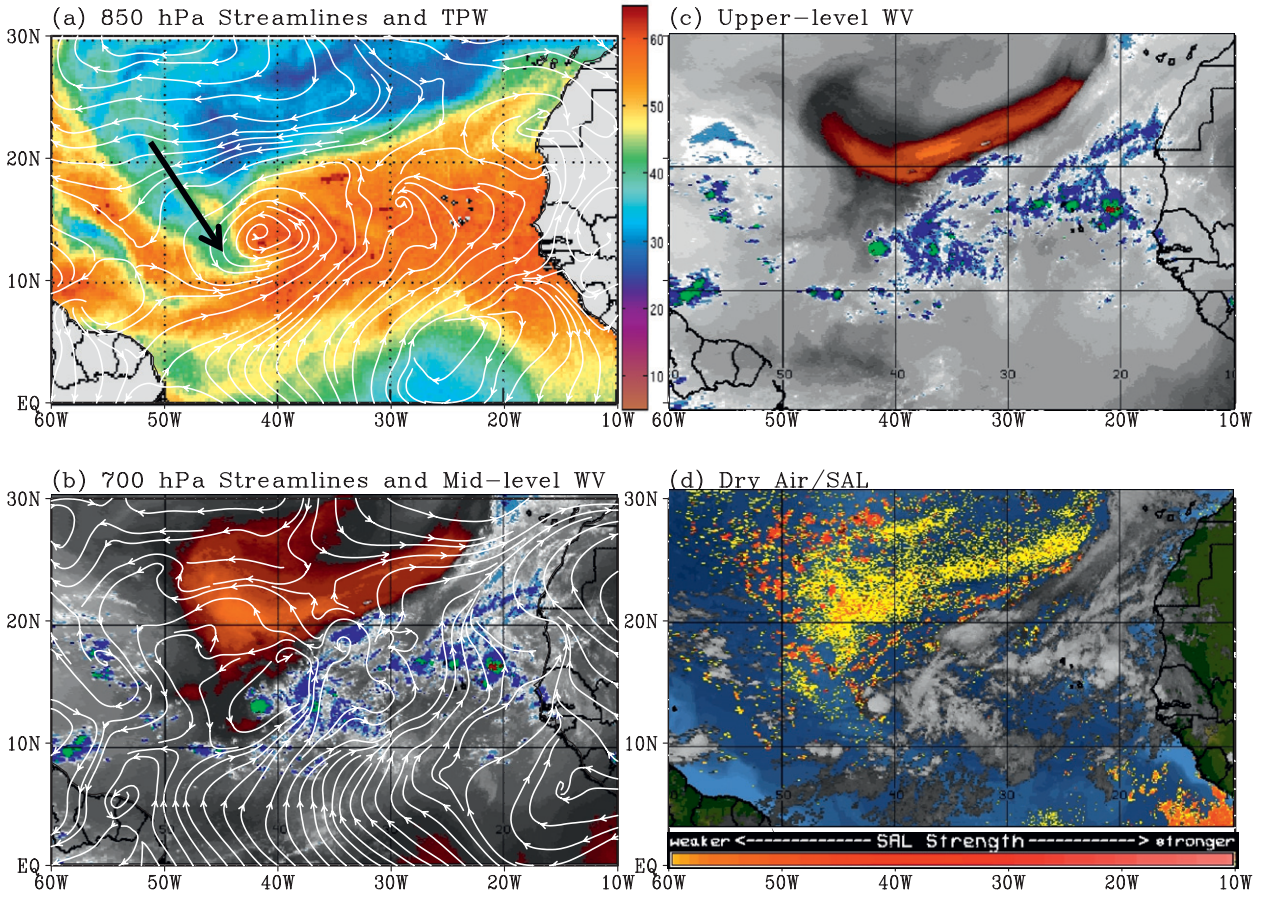

FIG. 14. (a) MIMIC–TPW and 850-hPa streamlines in the comoving frame (translation speed: -4.5 m s^{-1}), (b) enhanced midlevel water vapor and 700-hPa streamlines in the comoving frame, (c) enhanced upper-level water vapor, and (d) the dry air–SAL in the lower atmosphere at 1800 UTC 18 Sep. Yellow to red shading in (d) highlights the presence of dry and/or dusty air in the lower atmosphere (~600–850 hPa). The black arrow in (a) points to the dry air that is apparently intruding into the pouch.

study suggests that a moist and diabatically active wave pouch extending from 700 hPa down to the boundary layer is a necessary and highly favorable condition for tropical cyclone formation within an easterly wave.

Illustrative examples for each scenario were presented. The evolution of the pre-Fred disturbance suggests that persistent convection can stimulate the downward progression of a wave pouch in the presence of a low-level relative flow. The pregenesis evolution of Tropical Storm Erika shows that a deep pouch formed from the interaction of an African easterly wave with the intertropical convergence zone (ITCZ).

On the other hand, the fourth wave evolution scenario above suggests that a deep pouch by itself does not guarantee the formation of a tropical cyclone. The evolution of PG26L suggests that the dry air intrusion at the mid–upper levels can suppress tropical cyclone formation. We envision four main scenarios of dry air intrusionn–entrainment. One takes place in the mid–upper troposphere, where the wave remains open. Another scenario occurs when a large-sized pouch extends into the SAL (or other dry air mass) and advects dry air from the north. A third one is due to the divergent component of the flow, which induces an opening of the wave pouch and allows influx from the environment. A fourth scenario is associated with the small-scale convective vortices within and near the periphery of the pouch that can entrain dry air from outside the pouch via chaotic advection. The last scenario is not observable with the large-scale analyses. However, the first three scenarios may be tested with the large-scale analyses and may have taken place in PG26L. Analysis of satellite observations with GFS analysis data suggests also that dry air is not necessarily associated with the SAL. Instead, the midlevel dry air intrusion in PG26L is likely associated with a midlatitude frontal system and the large-scale subsidence.

Another detrimental factor discussed in section 4 is strong vertical shear. Strong vertical shear disrupts

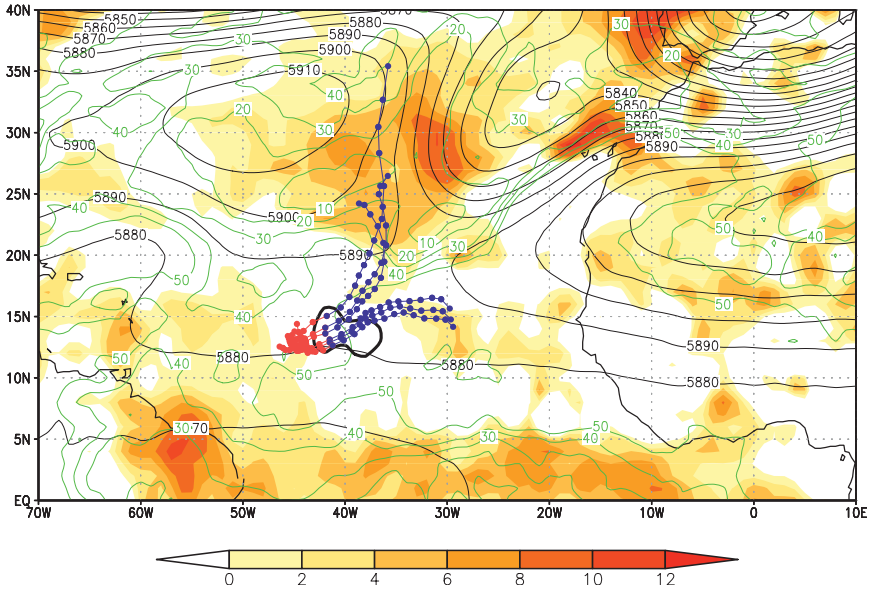

FIG. 15. The 500-hPa geopotential height (black contours with the interval of 10 m), RH (green contours with contour interval of 10%; values >50% are not shown), and vertical velocity in the isobaric coordinates (shading; 10^{-2} Pa s^{-1}) temporally averaged between 0000 UTC 17 Sep and 0000 UTC 24 Sep 2009. The thick black contour delineates the region of positive OW at 700 hPa, indicating the location of the wave pouch. Six particles are selected to show 3-day backward (blue) and 2-day forward (red) trajectories, starting at 1800 UTC 18 Sep, at 500 hPa in the western part of the wave, where the intrusion of dry air into the pouch is hypothesized to have occurred.

convection organization and hinders tropical cyclone formation. On the other hand, a wave pouch may be more resilient to vertical shear than a tropical storm as suggested in the evolution of PG24L. A pouch can persist a long time in the presence of strong vertical shear and may spawn a tropical cyclone later after it propagates to a more favorable environment. Besides dry air intrusion and strong vertical shear, there may be other detrimental factors, such as a lack of sufficient CAPE and presence of strong convective inhibition (CIN) within the wave pouch. All these can prevent sustained convection within the wave pouch (i.e., diabatic activation of the wave pouch), and thus hinder tropical cyclone formation.

Our diagnosis of the pouch kinematics is mainly based on the model analysis data. While a synoptic-scale wave may be captured by the analysis, the details of the subsynoptic vorticity structure are generally insufficiently resolved by the coarse-resolution analysis data, which are strongly influenced by the ''first guess'' stage of the data assimilation process. The cumulus parameterization employed in a global model introduces additional uncertainties to the analysis data, especially to the moisture and divergence fields. It is necessary to examine how well global models represent and forecast the pouch structure and evolution. An analysis of the PREDICT field data is currently under way to address these issues.

The road ahead

As noted in the introduction, an important question in tropical cyclone research is what controls the development or nondevelopment of a wave. This is a fundamental issue for tropical cyclogenesis, as it helps to differentiate developing waves from nondeveloping waves. A tropical cyclone is a meso-β-scale vortex, residing between the synoptic-scale waves and the meso-γ-scale convective processes. There generally is downscale enstrophy cascade from the synoptic scale to the meso-β scale and an upscale energy cascade from the convective scale (meso-γ scale) to the meso-β scale. In this sense, tropical cyclogenesis can be regarded as a combination of the large-scale downscaling and convective-scale upscaling processes. On the other hand, we believe that occurrence of sustained convection inside of a wave pouch is largely controlled by the meso-α- and synoptic-scale conditions. A deep wave pouch with warm SST, weak vertical shear, abundant moisture, and convective instability (sufficient CAPE and small CIN) is likely a sufficient condition for sustained convection and tropical cyclone formation within a synoptic-scale wave disturbance. Although convective processes limit the predictability of the tropical

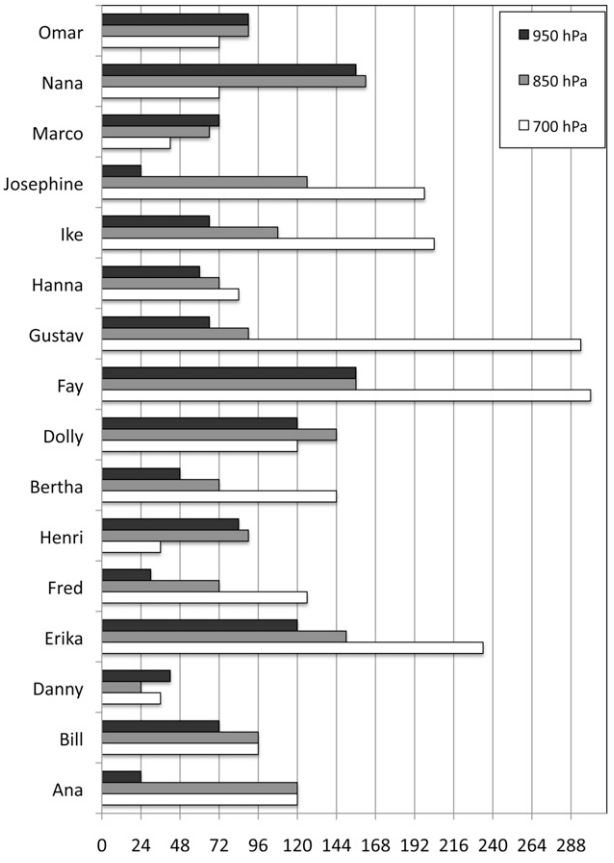

FIG. 16. Summary of the 2008/09 named Atlantic tropical storms originating from monochromatic easterly waves. The ordinate shows the storm names, and the abscissa indicates how many hours *prior to genesis* a pouch formed at 700 hPa (white bars), 850 hPa (gray bars), and 950 hPa (black bars).

cyclone formation (in particular, the genesis time), diagnoses of the large-scale environmental flow and synoptic-scale wave disturbances in the marsupial framework help us better understand the Lagrangian evolution of the precursor disturbances and differentiate developing versus nondeveloping waves.

Our study advocates strongly that one should track waves, instead of short-lived convection, when examining the evolution of a precursor disturbance. The OW parameter was shown to be a useful variable, as a positive OW region (as defined herein) highlights the flow that is shape preserving and favorable for rotational organization of deep convection and vorticity aggregation. On the other hand, OW (and also vorticity) in high-resolution data, such as ECMWF 25-km resolution analysis data, typically highlights the intense mesoscale vortices within the wave pouch and does not by itself provide adequate information on the kinematics of the meso-α-scale wave pouch, which can only be revealed by diagnosing streamlines in the wave-relative frame.

The results reported here are admittedly based on a limited number of storms. More storms and waves need to be examined 1) to further test the hypothesis that a deep pouch in the lower troposphere with other large-scale favorable conditions (warm SST, weak vertical wind shear, abundant moisture, and convective instability) is a sufficient condition for tropical cyclone formation within a synoptic-scale wave disturbance; 2) to identify the key processes for development or nondevelopment of a wave disturbance; 3) and to better understand the impacts of the large-scale environment on a wave pouch at the pregenesis stage. The authors hope that this study will stimulate further work on these important issues. A study based on a large sample size is under way, and the results will be reported in due course.

Acknowledgments. This research was supported by the National Science Foundation Grants ATM-1016095, AGS-1016095, AGS-1118429, AGS-0733380, and ATM-0733380. The real-time wave tracking in summer 2009 was a true team effort. We thank Mark Boothe, Robert LeeJoice, and Paul McCrone for their contribution to the daily wave tracking, NRL/Monterey for making satellite imagery available, and Dr. Jiann-Gwo Jiing for providing the IR Hovmöller diagram. We gratefully acknowledge Dr. Timothy Dunkerton for stimulating discussions during the dry run and two anonymous reviewers for their helpful comments. Figure 1 is courtesy of Timothy Dunkerton. The GFS data are from the NCAR CISL Research Data Archive (RDA).

REFERENCES

Bracken, W. E., and L. F. Bosart, 2000: The role of synoptic-scale flow during tropical cyclogenesis over the North Atlantic Ocean. *Mon. Wea. Rev.,* **128,** 353–376.

Braun, S. A., 2010: Reevaluating the role of the Saharan air layer in Atlantic tropical cyclogenesis and evolution. *Mon. Wea. Rev.,* **138,** 2007–2037.

Carlson, T. N., 1969: Synoptic histories of three African disturbances that developed into Atlantic hurricanes. *Mon. Wea. Rev.,* **97,** 256–276.

Davis, C. A., and L. F. Bosart, 2003: Baroclinically induced tropical cyclogenesis. *Mon. Wea. Rev.,* **131,** 2730–2747.

DeMaria, M., J. A. Knaff, and B. H. Connell, 2001: A tropical cyclone genesis parameter for the tropical Atlantic. *Wea. Forecasting,* **16,** 219–233.

Diaz, H. F., T. N. Carlson, and J. M. Prospero, 1976: A study of the structure and dynamics of the Saharan air layer over the northern equatorial Atlantic during BOMEX. NOAA/National Hurricane and Experimental Meteorology Laboratory Tech. Memo. ERL WMPO-32, 61 pp.

Drazin, P. G., and R. S. Johnson, 1989: *Solitons: An Introduction*. Cambridge University Press, 226 pp.

Dunion, J. P., and C. S. Velden, 2004: The impact of the Saharan air layer on Atlantic tropical cyclone activity. *Bull. Amer. Meteor. Soc.,* **85,** 353–365.

Dunkerton, T. J., M. T. Montgomery, and Z. Wang, 2009: Tropical cyclogenesis in a tropical wave critical layer: Easterly waves. *Atmos. Chem. Phys.,* **9,** 5587–5646.

Fang, J., and F. Zhang, 2010: Initial development and genesis of Hurricane Dolly (2008). *J. Atmos. Sci.,* **67,** 655–672.

Frank, N. L., 1970: Atlantic tropical systems of 1969. *Mon. Wea. Rev.,* **98,** 307–314.

Fujiwhara, S., 1921: The mutual tendency towards symmetry of motion and its application as a principle in meteorology. *Quart. J. Roy. Meteor. Soc.,* **47,** 287–293.

Goldenberg, S. B., and L. J. Shapiro, 1996: Physical mechanisms for the association of El Niño and West African rainfall with Atlantic major hurricane activity. *J. Climate,* **9,** 1169–1187.

Gray, W. M., 1968: Global view of the origin of tropical disturbances and storms. *Mon. Wea. Rev.,* **96,** 669–700.

——, 1998: The formation of tropical cyclones. *Meteor. Atmos. Phys.,* **67,** 37–69.

Hendricks, E. A., and M. T. Montgomery, 2006: Rapid scan views of convectively generated mesovortices in sheared Tropical Cyclone Gustav (2002). *Wea. Forecasting,* **21,** 1041–1050.

Holton, J. R., 2004: *An Introduction to Dynamic Meteorology*. 4th ed. Academic Press, 535 pp.

Hopsch, S. B., C. D. Thorncroft, and K. R. Tyle, 2010: Analysis of African easterly wave structures and their role in influencing tropical cyclogenesis. *Mon. Wea. Rev.,* **138,** 1399–1419.

James, R. P., and P. M. Markowski, 2010: A numerical investigation of the effects of dry air aloft on deep convection. *Mon. Wea. Rev.*, **138,** 140–161.

Jones, S. C., 1995: The evolution of vortices in vertical shear: Initially barotropic vortices. *Quart. J. Roy. Meteor. Soc.,* **121,** 821–851.

Karyampudi V. M., and Coauthors, 1999: Validation of the Saharan dust plume conceptual model using lidar, Meteosat, and ECMWF data. *Bull. Amer. Meteor. Soc.,* **80,** 1045–1075.

Kerns, B., and E. Zipser, 2009: Four years of tropical ERA-40 vorticity maxima tracks. Part II: Differences between developing and nondeveloping disturbances. *Mon. Wea. Rev.,* **137,** 2576–2591.

McBride, J. L., and R. Zehr, 1981: Observational analysis of tropical cyclone formation. Part II: Comparison of nondeveloping versus developing systems. *J. Atmos. Sci.,* **38,** 1132–1151.

McWilliams, J. C., 1984: The emergence of isolated coherent vortices in turbulent flow. *J. Fluid Mech.,* **146,** 21–43.

——, 2006: *Fundamentals of Geophysical Fluid Dynamics*. Cambridge University Press, 266 pp.

Montgomery, M. T., L. L. Lussier III, R. W. Moore, and Z. Wang, 2010a: The genesis of Typhoon Nuri as observed during the Tropical Cyclone Structure 2008 (TCS-08) field experiment – Part 1: The role of the easterly wave critical layer. *Atmos. Chem. Phys.,* **10,** 9879–9900.

——, Z. Wang, and T. J. Dunkerton, 2010b: Intermediate and high resolution numerical simulations of the transition of a tropical wave critical layer to a tropical depression. *Atmos. Chem. Phys.,* **10,** 10 803–10 827.

——, and Coauthors, 2012: The Pre-Depression Investigation of Cloud Systems in the Tropics (PREDICT) experiment: Scientific basis, new analysis tools, and some first results. *Bull. Amer. Meteor. Soc.,* **93,** 153–172.

Pedlosky, J., 1987. *Geophysical Fluid Dynamics*. 2nd ed. Springer-Verlag, 710 pp.

Peng, M. S., B. Fu, T. Li, and D. E. Stevens, 2012: Developing versus nondeveloping disturbances for tropical cyclone formation. Part I: North Atlantic. *Mon. Wea. Rev.,* **140,** 1047–1066.

Pytharoulis, I., and C. Thorncroft, 1999: The low-level structure of African easterly waves in 1995. *Mon. Wea. Rev.,* **127,** 2266–2280.

Raymond, D. J., and C. López Carrillo, 2010: The vorticity budget of developing Typhoon Nuri (2008). *Atmos. Chem. Phys. Discuss.,* **10,** 16 589–16 635, doi:10.5194/acpd-10-16589-2010.

Reasor, P. D., M. T. Montgomery, and L. D. Grasso, 2004: A new look at the problem of tropical cyclones in vertical shear flow: Vortex resiliency. *J. Atmos. Sci.,* **61,** 3–22.

Reed, R. J., D. C. Norquist, and E. E. Recker, 1977: The structure and properties of African wave disturbances as observed during phase III of GATE. *Mon. Wea. Rev.,* **105,** 317–333.

——, A. Hollingsworth, W. A. Heckley, and F. Delsol, 1988a: An evaluation of the ECMWF operational system in analyzing and forecasting easterly wave disturbances over Africa and the tropical Atlantic. *Mon. Wea. Rev.,* **116,** 824–865.

——, E. Klinker, and A. Hollingsworth, 1988b: The structure and characteristics of African easterly wave disturbances as determined from the ECMWF Operational Analysis/Forecast System. *Meteor. Atmos. Phys.,* **38,** 22–33.

Reznik, G. M., and W. K. Dewar, 1994: An analytical theory of distributed axisymmetric barotropic vortices on the β plane. *J. Fluid Mech.,* **269,** 301–321.

Ross, R. S., T. N. Krishnamurti, S. Pattnaik, and A. Simon, 2009: Energy transformation and diabatic processes in developing and nondeveloping African easterly waves observed during the NAMMA project of 2006. *Wea. Forecasting,* **24,** 1524–1548.

Smith, R. K., and W. Ulrich, 1993: Vortex motion in relation to the absolute vorticity gradient of the environment. *Quart. J. Roy. Meteor. Soc.,* **119,** 207–215.

——, ——, and G. Dietachmayer, 1990: A numerical study of tropical cyclone motion using a barotropic model. Part I. The role of vortex asymmetries. *Quart. J. Roy. Meteor. Soc.,* **116,** 337–362.

Thorncroft, C. D., and B. J. Hoskins, 1994: An idealized study of African easterly waves. I: A linear view. *Quart. J. Roy. Meteor. Soc.,* **120,** 953–982.

Vizy, E. K., and K. H. Cook, 2009: Tropical storm development from African easterly waves in the eastern Atlantic: A comparison of two successive waves using a regional model as part of NASA AMMA 2006. *J. Atmos. Sci.,* **66,** 3313–3334.

Wang, Z., M. T. Montgomery, and T. J. Dunkerton, 2009: A dynamically-based method for forecasting tropical cyclogenesis location in the Atlantic sector using global model products. *Geophys. Res. Lett.,* **36,** L03801, doi:10.1029/2008GL035586.

——, ——, and ——, 2010a: Genesis of pre–Hurricane Felix (2007). Part I: The Role of the wave critical layer. *J. Atmos. Sci.,* **67,** 1711–1729.

——, ——, and ——, 2010b: Genesis of pre–Hurricane Felix (2007). Part II: Warm core formation, precipitation evolution, and predictability. *J. Atmos. Sci.,* **67,** 1730–1744.

Weiss, J., 1991: The dynamics of enstrophy transfer in two-dimensional hydrodynamics. *Physica D,* **48,** 273–294.

Wimmers, A. J., and C. S. Velden, 2007: MIMIC: A new approach to visualizing satellite microwave imagery of tropical cyclones. *Bull. Amer. Meteor. Soc.,* **88,** 1187–1196.

Zawislak, J., and E. J. Zipser, 2010: Observations of seven African easterly waves in the east Atlantic during 2006. *J. Atmos. Sci.,* **67,** 26–43.

Zipser, E. J., and Coauthors, 2009: The Saharan air layer and the fate of African easterly waves—NASA's AMMA field study of tropical cyclogenesis. *Bull. Amer. Meteor. Soc.,* **90,** 1137–1156.